An Artificial Rabbits' Optimization to Allocate PVSTATCOM for Ancillary Service Provision in Distribution Systems

Mostafa Elshahed [1,2,*], Mohamed A. Tolba [3,4], Ali M. El-Rifaie [5,*], Ahmed Ginidi [6], Abdullah Shaheen [6] and Shazly A. Mohamed [7]

1   Electrical Engineering Department, Engineering and Information Technology College,
     Buraydah Private Colleges, Buraydah 51418, Saudi Arabia
2   Electrical Power Engineering Department, Faculty of Engineering, Cairo University, Giza 12613, Egypt
3   Reactors Department, Nuclear Research Center, Egyptian Atomic Energy Authority, Cairo 11787, Egypt
4   Electrical Power Systems Department, National Research University "MPEI", 111250 Moscow, Russia
5   College of Engineering and Technology, American University of the Middle East, Egaila 54200, Kuwait
6   Department of Electrical Power Engineering, Faculty of Engineering, Suez University, Suez 43533, Egypt
7   Electrical Engineering Department, Faculty of Engineering, South Valley University, Qena 83523, Egypt
*   Correspondence: mostafa.elshahed@bpc.edu.sa (M.E.); ali.el-rifaie@aum.edu.kw (A.M.E.-R.)

Abstract: Attaining highly secure and safe operation of the grid with acceptable voltage levels has become a difficult issue for electricity companies that must adopt remedial actions. The usage of a PV solar farm inverter as a static synchronous compensator (or PVSTATCOM device) throughout the night has recently been proposed as a way to enhance the system performance. In this article, the novel artificial rabbits' optimization algorithm (AROA) is developed for minimizing both the daily energy losses and the daily voltage profile considering different 24 h loadings. The novel AROA is inspired from the natural surviving strategies of rabbits. The novel AROA is tested on a typical IEEE 33-node distribution network including three scenarios. Different scenarios are implemented considering PV/STATCOM allocations throughout the day. The effectiveness of the proposed AROA is demonstrated in comparison to differential evolution (DE) algorithm and golden search optimization (GSO). The PVSTATCOM is adequately allocated based on the proposed AROA, where the energy losses are greatly reduced with 54.36% and the voltage deviations are greatly improved with 43.29%. Moreover, the proposed AROA provides no violations in all constraints while DE fails to achieve these limits. Therefore, the proposed AROA shows greater dependability than DE and GSO. Moreover, the voltage profiles at all distribution nodes all over the daytime hours are more than the minimum limit of 95%.

Keywords: artificial rabbits' optimization; ancillary service provision; distribution systems; PVSTATCOM allocation

MSC: 37N40; 65K10

1. Introduction

Renewable energy (RE) is a significant resource of clean energy transitions to keep the increase in worldwide temperatures below 1.5 °C. In 2022, the annual capacity of RE is likely to be about 340 GW. In addition, RE needs to develop faster to increase from almost 29% in 2021 to more than 60% by 2030. In 2021, RE increased by almost 7%, a record 522 TWh growth, with wind and solar PV resources together contributing almost 90% of this growth [1]. Modern electrical transmission and distribution networks have been requesting innovative services and solutions to fulfill the increased demand for electricity brought on by urbanization, technological advancements, and the pursuit of a better quality of life. Distributed energy resources (DER), notably photovoltaic DERs, has been supporting active generated power in distribution networks more and more.

However, it is getting harder to supply the need for reactive electricity [2–4]. In recent decades, traditional energy has significantly harmed the environment. In order to promote environmental preservation, suitable renewable sources have received considerable focus in recent times. Sunlight has become one of the most economical renewable resources owing to its own global affordability and cleaning. In many different sectors, PVDER systems perform a vital part in the global growth of renewable energy due to the fact that they can easily transform solar energy into electrical energy [5,6]. The mathematical models of such PVDER systems are usually presented through single, double, and triple diode models. In such systems, the results from swarming and evolution optimizers were underdeveloped because of the nonlinearity and complexity of the PV parameter identification as indicated by a hybridized rat swarm optimization algorithm and pattern search [7] and a modified salp swarm algorithm [8]. Furthermore, PVDER systems are integrated with batteries which give higher opportunities to supply electricity at night. Lithium-ion batteries (LIBs) are efficient and reliable types with several adequate estimations of their state of health (SOH) based on electrochemical impedance spectroscopy (EIS) [9,10].

Transmission system operators (TSOs) dictated the preventive grid codes' requirements to overcome the difficulties that may appear due to the high increase of RE with an intermittent nature [2]. Consequently, with high penetration of RE, the power systems must comply with the grid codes during any disturbances [11]. For example, the reactive power capabilities must be maintained during and after any disturbances that may occur to keep the integration of RE. For this purpose, the FACTS devices are usually used to inject the reactive current for voltage support. STATCOM is the most commonly used as it is more efficient compared to other FACTS devices for reactive power compensation and incorporation of renewable energy [12]. According to the IEC 60050-617, ancillary services are services necessary for the operation of an electrical power system provided by the system operator and/or users of the power system [13]. Distributed generation (DG) can offer ancillary services including voltage regulation, congestion management, frequency control, black start, reduced power losses, enhanced power quality, and islanded operation [14,15]. Flexible sources relying on grid-connected inverters are able to meet a large portion of the reactive power demand in distribution systems [16]. This technology creates new commercial prospects in the industry. For instance, PVDER inverters rely on solar irradiation; as a result, they are inactive for the majority of the day. Their unused capacity has the potential to serve the network with a variety of ancillary services, such as reactive power supplies [17].

Smart inverters represent a standard move in the incorporation of DER [18]. These inverters can achieve both reactive and active power control during converting DC power to AC power including voltage regulation, power factor control, active power controls, ramp-rate controls, fault ride-through, frequency control, etc. [18]. However, if the voltage is at a low level during the nighttime, the smart invert must disconnect [19]. An exclusive application of STATCOM in PV solar farms for supporting different grid functions during daytime and nighttime was proposed in [20,21]. STATCOM offers a dynamic reactive power compensation with a high fast response time and generates the rated reactive current at very low voltages [19]. The application of PV solar farms as STATCOM, named PVSTATCOM, was established for improving the power transmission capacity during night and day [22,23]. In [22], PVSTATCOM has been applied to enhance the performance of the distribution systems where voltage control during critical system needs can be utilized. In that study, a dynamic reactive power compensator was activated via smart PV inverter in which the PV inverter was controlled as STATCOM. In [23], PVSTATCOM with STATCOM interface control was employed for controlling steady-state voltage and temporary over voltages in a practical distribution feeder. The main purpose of the STATCOM installations in that feeder was successfully achieved where all of the identified voltage problems have been satisfactorily resolved in accordance with the utility grid code [24]. In [25], PVSTATCOM has been installed in power transmission systems in order to provide power oscillation damping due to a system disturbance. In this study, the solar farm ramps

up active power output to its pre-disturbance amount as soon as power oscillations are dampened, maintaining the damping feature active. As a result, restoration happens a lot quicker than what the grid codes specify. In [26], a dynamic performance of a PVSTATCOM has been investigated for improving power quality in a grid-connected mode and enabling low voltage ride through capability through the injection of active and reactive powers to enhance the voltages through the system under abnormal grid conditions. In [27], the concept of PVSTATCOM focuses on the enhancement of the dynamic performance of the IEEE 33-bus distribution system. In this study [27], under voltage sag or post-fault situations, PVSTATCOM's quick reactive power adjustment has helped the voltage recovery operations. In [28], distributed generating units have been optimally jointed with electric vehicle charging stations in distribution networks. A realistic metropolitan region in China that is served by a 31-bus distribution system has been used in this work [28] by implementing linearized power flow models and an accurate second order conic relaxation.

In [29], Distribution-STATCOM (D-STATCOM) has been allocated, based on particle swarm optimization (PSO) and the Monte Carlo simulation (MCS) method [30] in both mesh and radial distribution systems in order to reduce the power losses and improve the voltage deviations considering different RESs and their probabilistic, uncertain natures. In [31], solar-PV and STATCOM have been allocated via the PSO algorithm to minimize the overall losses and improve the voltage profile of the IEEE 30 bus distribution system. Generally, the PVSTATCOM can greatly help in adequate integration to overcome several challenges in power systems [32].

Lately, Wang et al. [33] introduced a unique artificial rabbits' optimization algorithm (AROA) that takes cues from the natural surviving strategies of rabbits, such as detour eating and random concealment. This primary driving force of the AROA emphasizes the aspects that make it useful in addressing various optimization problems. A portion detour forages for food; the rabbit gets compelled to consume the grass close to other nests nearby in order to prevent predators locating its nest. Additionally, a rabbit can choose whichever of its personal homes to escape to at random using the randomized hiding strategy, which could reduce the possibility of it being captured by predators. Rabbits' energy could also decline such that it would make them abandon their deliberate foraging style in favor of haphazard concealment. In this paper, a novel AROA is developed for minimizing the daily energy losses and the daily voltage profile considering different 24 h loadings. Its relevance is tested on a typical IEEE 33-node distribution network. The simulation applications are conducted for PVDERs allocation individually and simultaneous PVSTATCOM allocation is conducted to minimize the considered objective function through the day. The effectiveness of the proposed AROA is demonstrated in comparison to differential evolution (DE) algorithms.

The key contributions of the paper can be summarized as follows:

- A novel AROA has been developed for simultaneous PVSTATCOM allocation in distribution systems;
- Daily energy losses and voltage profiles considering different 24 h loadings have been taken into consideration in the objective function and constraints;
- Higher effectiveness of the proposed AROA versus DE and GSO in minimizing the energy losses and voltage profile deviations and maintaining all the operational constraints;
- Moreover, the proposed AROA shows lower computational time compared to DE and GSO;
- It is noticed from this scenario that the losses and voltage deviations are reduced when using the STATCOM with PV.

The remaining sections of this paper involve the following. Section 2 highlights the mathematical model of the novel AROA, whilst Section 3 manifests the mathematical formulation of the PVSTATCOM allocation in distribution systems. Furthermore, the simulation results of the developed AROA for PVSTATCOM allocation in distribution systems considering different 24 h loadings are elaborated in Section 4, and the conclusions of this work are developed in Section 5.

2. AROA: Mathematical Model

The surviving strategies used by rabbits in reality are represented mathematically in an effective optimization model for the suggested AROA. Two emulated strategies—detour eating and haphazard hiding—are addressed in that manner. At first, the detour foraging tactic is simulated where the rabbit gets compelled to consume the grass surrounding other nests nearby in order to prevent predators from locating its home. At second, using the randomized hiding tactic, the chance that a rabbit would be captured by the enemies could well be reduced. At third, rabbits might also lose energy, that could force them to abandon their detour feeding approach in favour of an erratic hiding tactic [33].

Every iteration updates the population of the rabbits' position according to the criteria of the provided method, then it is subjected to the objective function's assessment. As the procedure continues, the search agents of the rabbit's positions, which represent the solutions, get better. In accordance with Equation (1), a randomized site within the searching space is appointed to every position in the beginning population:

$$Rb_i = LB + rand(1, dim) \times [UB - LB] \ i = 1 : N_{Rb} \tag{1}$$

where Rb_i denotes the location of each rabbit, UB and LB denote the upper and lower bounds of the design variables, N_{Rb} and dim are, correspondingly, the number of rabbits in the population and the number of the variables that are being evaluated.

2.1. Detour Forage Tactic

Each seeking rabbit chooses to switch positions with another seeking animal chosen randomly from the swarm and undertake distraction, as per the AROA's detour forage tactic. Mathematically, rabbits' detour forage is represented as:

$$NRb_k(iter + 1) = Rb_j(iter) + \left(Rb_k(iter) - Rb_j(iter)\right) \times Zm + NDS \times round\left(\frac{1}{2} \times \left(\frac{5}{100} + r_1\right)\right),$$
$$k, j = 1 : N_{Rb}, j \neq k \tag{2}$$

$$Zm = c \times \left(e - e^{\left(\frac{iter-1}{Iter_{max}}\right)^2}\right) \times \sin(2\pi r_2) \tag{3}$$

$$c(j) = \begin{cases} 1 \ if \ j = g(\psi) \\ 0 \ else \end{cases}, j = 1 : dim \ and \ \psi = 1 : [r_3, dim] \tag{4}$$

$$g = randperm(dim), \ n_1 \sim N(0,1) \tag{5}$$

where *iter* indicates to the current iteration, Rb_k and NRb_k are the old and new locations of the kth rabbit, *NDS* is the standard function related to normal distribution, *randperm* is a randomizing permutation function, r_1, r_2, and r_3 are three random numbers within range [0, 1], and $Iter_{max}$ represents the maximum iterations number.

2.2. Randomized Hiding Tactic

A rabbit frequently excavates a number of tunnels near its nest to serve as shelter when evading predators. The equation below is offered in this regard.

$$b_{k,j}(iter) = Rb_k(iter) \times (1 + H.G) \tag{6}$$

$$k = 1 : N_{Rb} \text{ and } j = 1 : dim \tag{7}$$

$$H = r_4 \times \frac{Iter_{\max} - iter + 1}{Iter_{\max}} \tag{8}$$

$$G(j) = \begin{cases} 1 \text{ if } j = k \\ 0 \text{ else} \end{cases} \quad j = 1 : dim \tag{9}$$

where r_4 seems to be a randomly chosen number between [0, 1], $b_{k,j}$ is the jth burrow of the kth rabbit, and H is the hiding value, which progressively falls from 1 to $1/Iter_{\max}$ as a function of the current iteration. These burrows are initially built in a rabbit's bigger surroundings based on this trait. The more iterations there are, the smaller this region becomes.

To remain, rabbits need to find a safe location to stay. They select a hole at random from those they must hide in to remain undetected. This randomized concealing technique can be described in the following algebraic equation:

$$NRb_k(iter + 1) = Rb_k(iter) + Zm \times \left(r_5 \times b_{k,j}(iter) - Rb_k(iter)\right) \quad k = 1 : N_{Rb} \tag{10}$$

The kth rabbit's location is altered as following if detour forage or randomly hiding are effective:

$$Rb_k(iter + 1) = \begin{cases} Rb_k(iter) & f(Rb_k(iter) \leq f(NRb_k(iter + 1)) \\ NRb_k(iter + 1) & f(Rb_k(iter) > f(NRb_k(iter + 1)) \end{cases} \tag{11}$$

2.3. Energy Decline

An energy component is taken into account while modelling the transition from the discovery process associated with detour forage to the exploitation stage characterized by randomized concealment. The energy factor (AF) can be defined as follows:

$$AF(iter) = 4 \times \ln\frac{1}{r} \times \left(1 - \frac{iter}{Iter_{\max}}\right) \tag{12}$$

The strategies listed previously could be combined in Figure 1 to show the key stages of the suggested AROA.
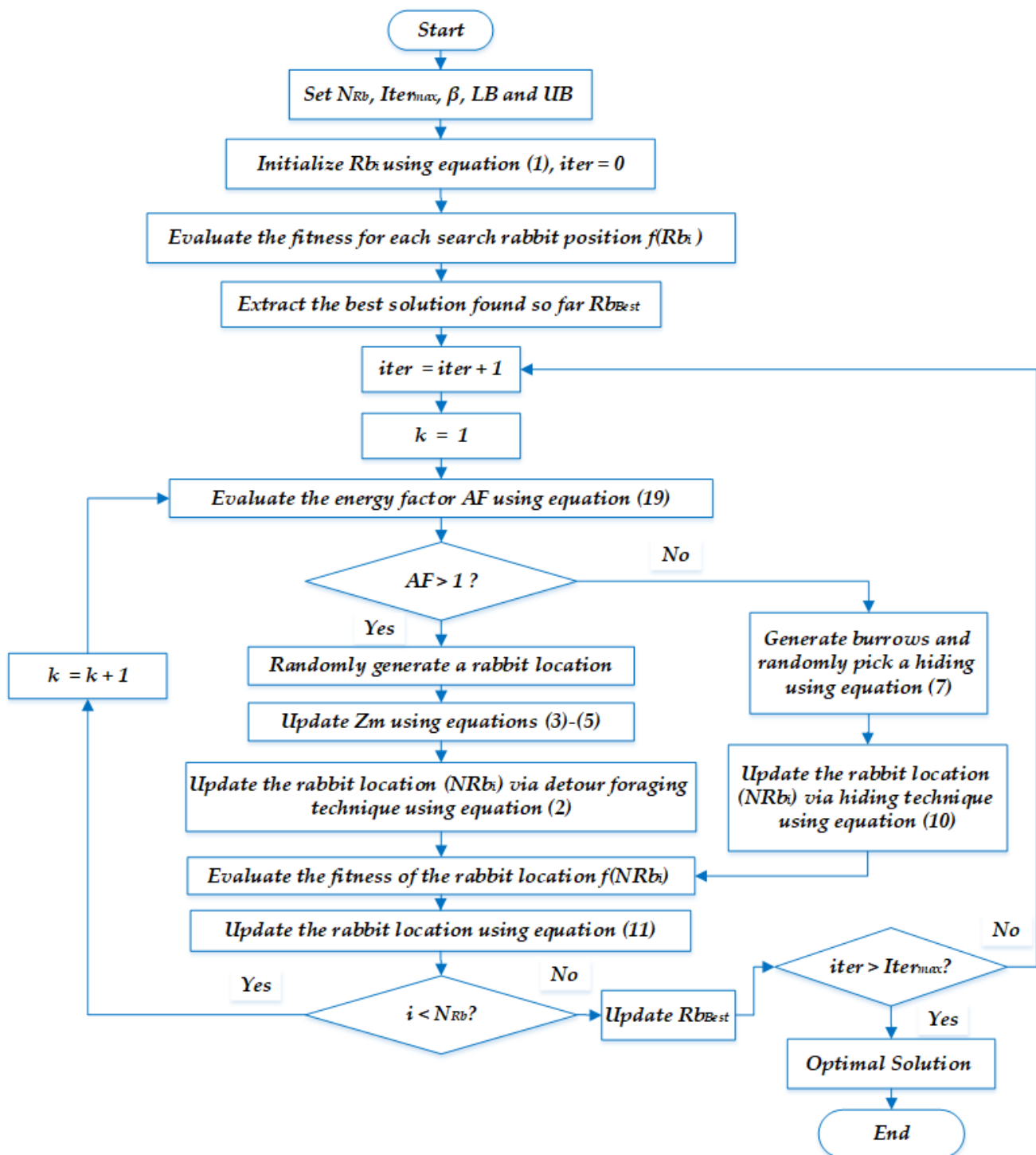
Figure 1. Main steps of the proposed AROA in solving real engineering optimization problems.

3. PVSTATCOM Allocation for Ancillary Service Provision in Distribution Systems

3.1. PVSTATCOM Model

A PVSTATCOM is a solar plant comprising a STATCOM, as shown in Figure 1, was used to control the voltage of a distribution electricity system that included solar power facilities [20]. During the night, when no actual power output from the PV units is taking place, the PV inverter was able to perform this role. The reactive power supplied from STATCOM controls the voltage at the point of common coupling (PCC) [34] when there is a three-phase fault, any little disruption, or a voltage sag or rise. Voltage regulation is

implemented throughout the day to significantly enhance the concept [35]. PVSTATCOM model was implemented as a voltage control with an auxiliary damping control to improve transient stability which is manifested in the power transfer limitation [36]. The results revealed that a PVSTATCOM is not only suitable in distribution networks, but it can also significantly increase the stable transmission limitations throughout the day and night, even while creating tens of MW of actual power [37]. Figure 2 depicts the topology of a PVSTATCOM instrument connected to an electricity network.
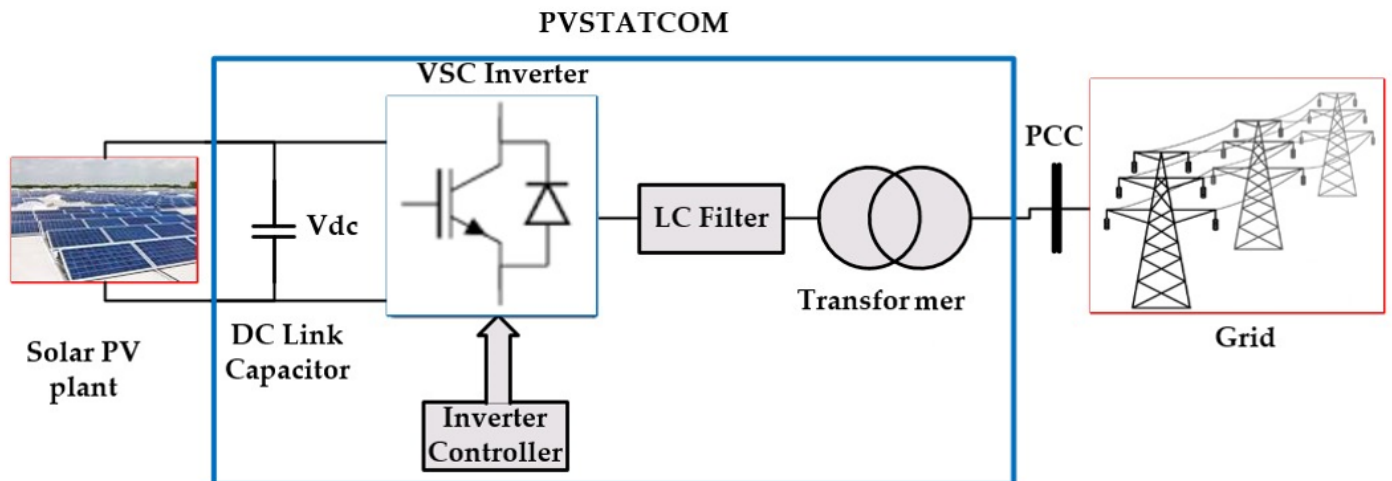
Figure 2. Configuration of PVSTATCOM device to be connected to an electrical power system [36].

In the PVSTATCOM model, the inverter's active current regulates the DC voltage. This component may be supplied by the solar panels during real power injections or by the reactive component of the injecting current for voltage regulating at the PCC. In this study, the PVSTATCOM's ability to inject active power during the day is taken into account together with its concurrent ability to absorb and inject reactive power during the day and night.

In order to integrate the PVSTATCOM model in the power distribution network, the whole balance constraints are modified at each hour. Therefore, the active and reactive power balance restrictions can be modelled as follows:

$$\left(P_s + \sum_{n=1}^{N_{PVSTATCOM}} P_{PVSTATCOM_n} = \sum_{k=1}^{N_{buses}} Pd_k + P_{losses} \right)_{h=1:24} \tag{13}$$

$$\left(Q_s + \sum_{n=1}^{N_{PVSTATCOM}} Q_{PVSTATCOM_n} = \sum_{k=1}^{N_{buses}} Qd_k + Q_{losses} \right)_{h=1:24} \tag{14}$$

where Ps is the total supplied active power from the substation, $P_{PVSTATCOMn}$ is the real power injection from PVSTATCOM to be installed at node (n), $N_{PVSTATCOM}$ is the number of installed PVSTATCOM systems, Pd_k is the active power demand at node (k), Plosses indicates the active power losses through the whole system, h refers to every hour through the day horizon, Qs is the total supplied reactive power from the substation, $Q_{PVSTATCOMn}$ is the reactive power absorption/injection from PVSTATCOM to be installed at node (n), Qd_k is the reactive power demand at node (k), and $Qlosses$ indicates the reactive power losses through the whole system.

3.2. PVSTATCOM Allocation for Ancillary Service Provision: Constraints and Objective

For PVSTATCOM allocation for ancillary service provision in distribution systems, the minimization of energy losses and voltage deviations on a daily basis are to be considered. Both targets are considered in a single objective model (*Obj*) to be minimized as in Equation (15).

$$Obj = \text{Min}(EL_D + VD_D) \tag{15}$$

where EL_D represents the energy losses per day and VD_D is the voltage deviation per day, which can be modeled as follows:

$$EL_D = \sum_{h=1}^{24} \left(\sum_{br=1}^{N_{branches}} I_{br}^2 . R_{br} \right) \tag{16}$$

$$VD_D = \sum_{h=1}^{24} \left(\sum_{j=1}^{N_{buses}} |1 - V_j| \right) \tag{17}$$

where $N_{branches}$ is the number of distribution branches, I_{br} is the current flow through each distribution branch (*br*), R_{br} is the resistance of each distribution branch (*br*), N_{buses} is the number of buses, and V_j is the voltage magnitude at each distribution node (*j*)

For this purpose, the ability of the PVSTATCOM to simultaneously absorb and inject reactive power during the day and night is taken into consideration along with its capacity to inject active power during the day. Therefore, the real and reactive power injection from PVSTATCOM, at each hour, to be installed at node (*n*), are to be maintained inside the candidate size which is indicated by $P_{PV,\max}$ and $Q_{STATCOM,\max}$, respectively.

$$(0 < P_{PVSTATCOM,n} \leq P_{PV,\max,n}) \quad \begin{matrix} h = 1:24 \\ n = 1:N_{PVSTATCOM} \end{matrix} \tag{18}$$

$$(0 < Q_{PVSTATCOM,n} \leq Q_{STATCOM,\max,n}) \quad \begin{matrix} h = 1:24 \\ n = 1:N_{PVSTATCOM} \end{matrix} \tag{19}$$

Moreover, the voltage at all distribution nodes and the current flow through all distribution branches should be maintained for all hours inside the permissible limits as follows [38]:

$$V_{j\min} < V_j < V_{j\max} \,\, _{\&h=1:24\&j=1:Nbuses} \tag{20}$$

$$I_{br} < I_{br\max} \,\, _{\&h=1:24\&br=1:Nbranches} \tag{21}$$

where $V_{j\min}$ and $V_{j\max}$ are the lower and higher limits of the voltage nodes which gives 5% permissible range and $I_{br\max}$ indicates the thermal capacity limit of the distribution branch.

Moreover, the penetration limit (K_p) of the *PV* resources should be considered with 60% of the total active power demand in the system as [39]:

$$([Pen_{Constraint} = (\sum_{i=1}^{N_{PVSTATCOM}} P_{PVSTATCOM} - K_P * \sum_{k=1}^{N_{buses}} P_{d_k})] \leq 0) \,\, \begin{matrix} h = 1:24 \\ \max peak demand \end{matrix} \tag{22}$$

The inequality constraints of Equations (18) and (19) are related to the control variables and consequently they are automatically handled via the AROA mechanism. On the other side, the inequality constraints of Equations (20)–(22) should be further addressed.

Therefore, any violation in one of these constraints is added with penalty terms to the objective function described in Equation (15), which is upgraded as follows:

$$Obj = EL_D + VD_D + K_1 * Viol_{V,\max} + K_2 * Viol_{V,\min} + K_3 * Viol_{br} + K_4 * Viol_{penetration} \tag{23}$$

where K_1, K_2, K_3, and K_4 are penalty coefficients which are set to very high value. The first two coefficients belong to the violation of voltage at the distribution nodes ($K_1 = K_2 = 10^4$), while K_3 belongs to the violation of current flow through the distribution branches ($K_3 = 10^3$) and K_4 belongs to the violation of the penetration limit ($K_4 = 10^3$).

$$Viol_{V,\max} = \begin{cases} \max(V_j) - V_{j,\max} \ if \ V_{j,\max} < V_j \\ 0, \quad else \end{cases} \tag{24}$$

$$Viol_{V,\min} = \begin{cases} V_{j,\min} - \min(V_j) \ if \ V_{j,\min} > V_j \\ 0, \quad else \end{cases} \tag{25}$$

$$Viol_{br} = \begin{cases} \max(I_{br}) - I_{br,\max} \ if \ I_{br,\max} < I_{br} \\ 0, \quad else \end{cases} \tag{26}$$

$$Viol_{penetration} = \begin{cases} Pen_{Constraint} \ if \ Pen_{Constraint} > 0 \\ 0, \quad else \end{cases} \tag{27}$$

4. Simulation Results

The suggested AROA's relevance is tested on a typical IEEE 33-node distribution network. This network has 32 distribution sections and 33 nodes (numbered from Z1 to Z32). The network one-line diagram for a system with a standard voltage of 12.66 kV is shown in Figure 3. The maximum reactive power limit of PVSTATCOM is ±1000 kVAr. For the proposed AROA, DE, and GSO, the parameters for scenarios 2 and 3 are 50 individuals in each population and 300 number of iterations. For DE, the mutation and crossover rates are equal to 0.5. For the nominal loading condition, the overall active (MW), reactive (MVAr), and apparent demands (MVA) are, respectively, 3.715, 2.3, and 4.369 [40].
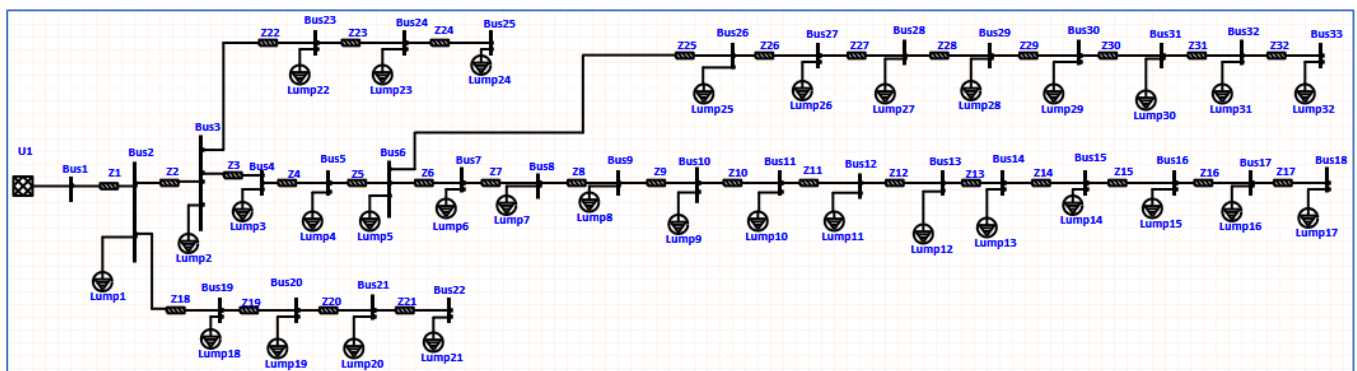

Figure 3. One-line configuration of standard IEEE 33-distribution system.

Three scenarios are investigated as follows:

Scenario 1, load flow is carried out for each loading hour;

Scenario 2, Application of the proposed AROA in comparison to DE for PV allocations, without STATCOM, to minimize the considered objective function (Equation (23));

Scenario 3, Simultaneous PVSTATCOM allocation to minimize the considered objective function (Equation (23)).

With AROA settings of 300 iterations and 50 search agents, scenarios 2 and 3 are both run. The node's voltage value should be constrained to 5% of the nominal voltage or less. The maximum number of PVDERs that can be installed is four. The maximum

capacity of each PVDER and STATCOM is 1 MW. Each load's power factor is maintained constant during the simulations, and all distribution nodes are assumed to possess the identical loading curve, as described in Figure 4. The model for load demands is constant power. From Figure 4, peak demand for the loading profile arrives around 12:00 p.m. and continues for 4 h, when 100% of the loading is in use.
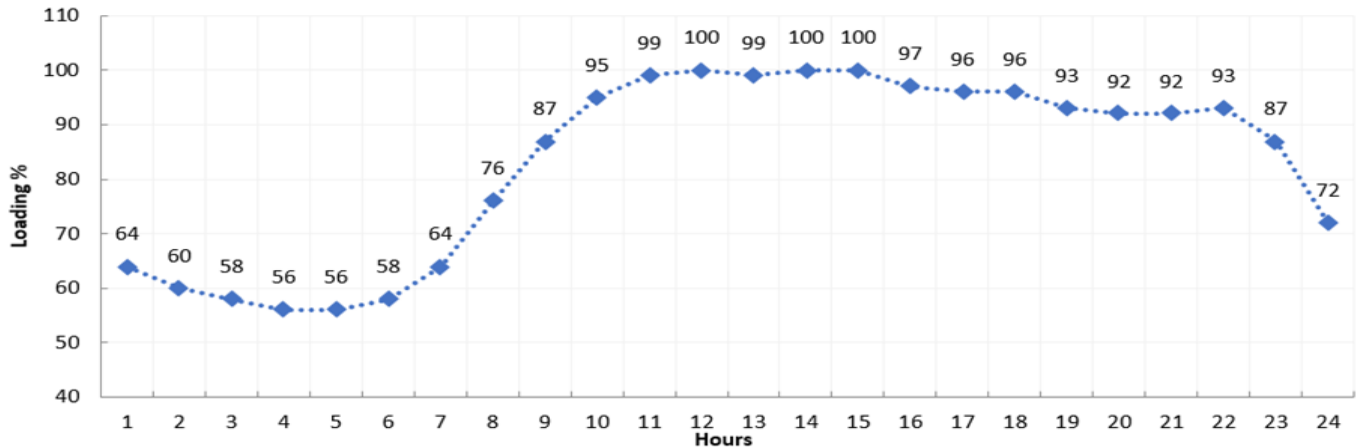

Figure 4. Hourly loading profile in percentage of the nominal condition [41].

4.1. First Scenario

In this scenario, load flow is carried out for each loading hour. Figure 5 describes the hourly voltage profile of all distribution nodes. As shown, the worst voltage profile is occurred at the peak loading conditions where the nodes 7–18 and 26–33 are suffered from undervoltage compared to the minimum limit of 95%. At peak consumption hours, the lowest voltage on the grid is 0.9131 p.u. and occurs at bus 18, as shown in Figure 5. Additionally, Figure 6 displays the hourly voltage deviations where the worst voltage deviations of 1.8118 are at peak loading and the best voltage deviations of 0.9785 are at low loading at 4:00–5:00 a.m. Moreover, Figure 7 illustrates the hourly active power losses. The active and reactive power flows through the distribution lines are required in order to supply the active and reactive power demands at all distribution buses. These flows pass through the resistance and the reactance of the distribution lines causes active and reactive power losses which are dependent of the square of the current flow through each segment.
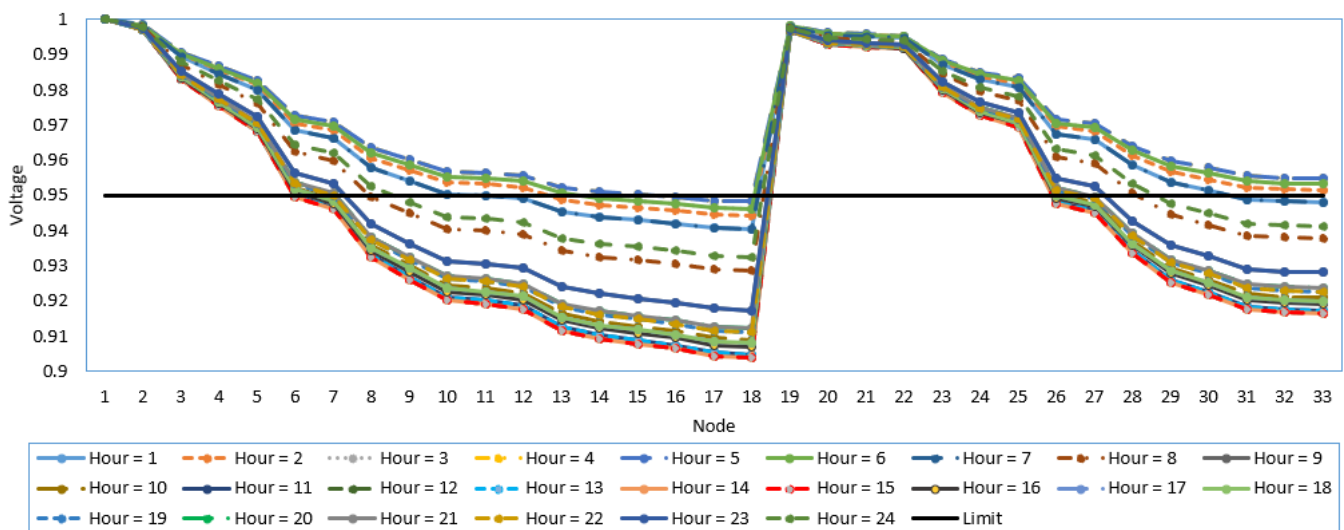

Figure 5. Hourly voltage profile for the first scenario for the IEEE 33-distribution system.
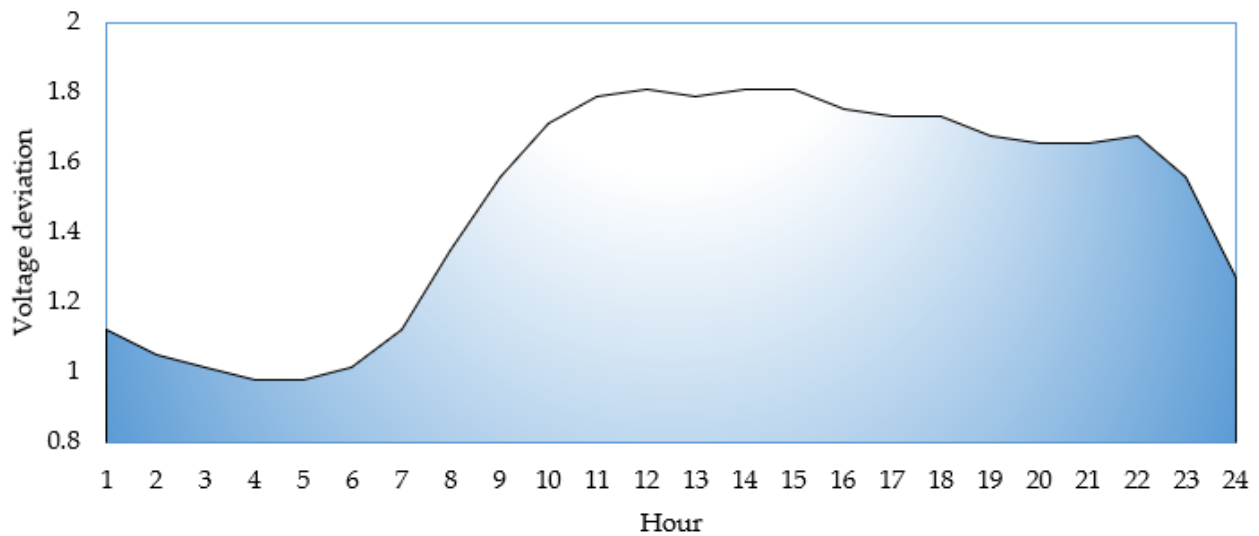
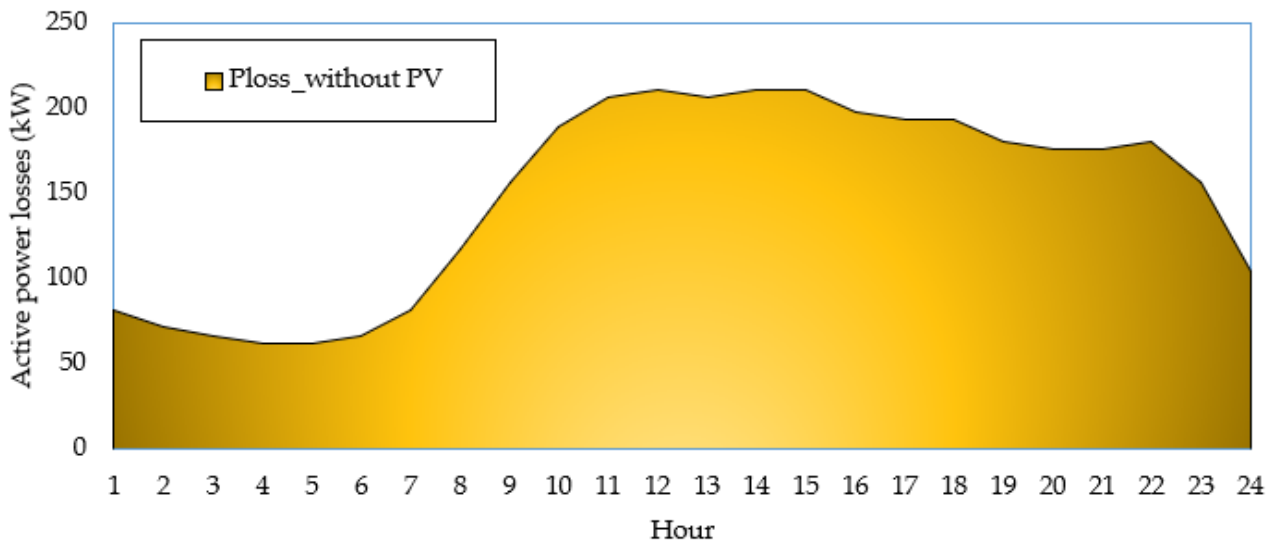**Figure 6.** Hourly voltage deviations for the first scenario for the IEEE 33-distribution system.

Figure 7. Hourly active power losses for the first scenario for the IEEE 33-distribution system.

4.2. Second Scenario

In this scenario, the proposed AROA is applied in comparison to DE for PV allocations, without STATCOM, to minimize the considered objective function (Equation (23)). The proposed AROA and DE are applied for this scenario. Table 1 shows that the allocations of PV without STATCOM, where the numbers of installed buses obtained by the AROA are 11, 17, and 31, and their corresponding PV sizes are 636, 844, and 971 kW, respectively. On the other side, the installed buses obtained by DE are 12, 31, and 18, and their corresponding PV sizes are 818, 936, and 969 kW, respectively. It can be noticed from this table that the objective of the proposed AROA is reduced to 5223.662 compared with 5224.216 that is achieved from DE. To illustrate the comparison between the AROA and DE, new parameters such as energy losses, voltage deviations, violations, and their corresponding objectives are developed for this scenario as depicted in Table 2. The convergence characteristics of DE and the AROA for this scenario is described in Figure 8. The figure shows that the AROA has excellent convergence characteristics compared with DE in obtaining the least objective without STATCOM.

Table 1. Allocations of PV without STATCOM for the second scenario for the IEEE 33-distribution system.

Items	DE	AROA
Installed buses	12	11
	31	17
	18	31
Regarding PV Size (kW)	818	636
	936	844
	696	971
Objective	5224.216	5223.662

Table 2. Corresponding energy losses, voltage deviations, and violations for the second scenario for the IEEE 33-distribution system.

Items	Initial	DE	AROA
Energy Losses (kWh/day)	3557.2479	2485.314	2482.624
Voltage deviations (p.u./day)	35.643	28.4277	28.4663
Violations	6912.71	2710.4729	2712.6
Objective	10505.6	5224.216	5223.662
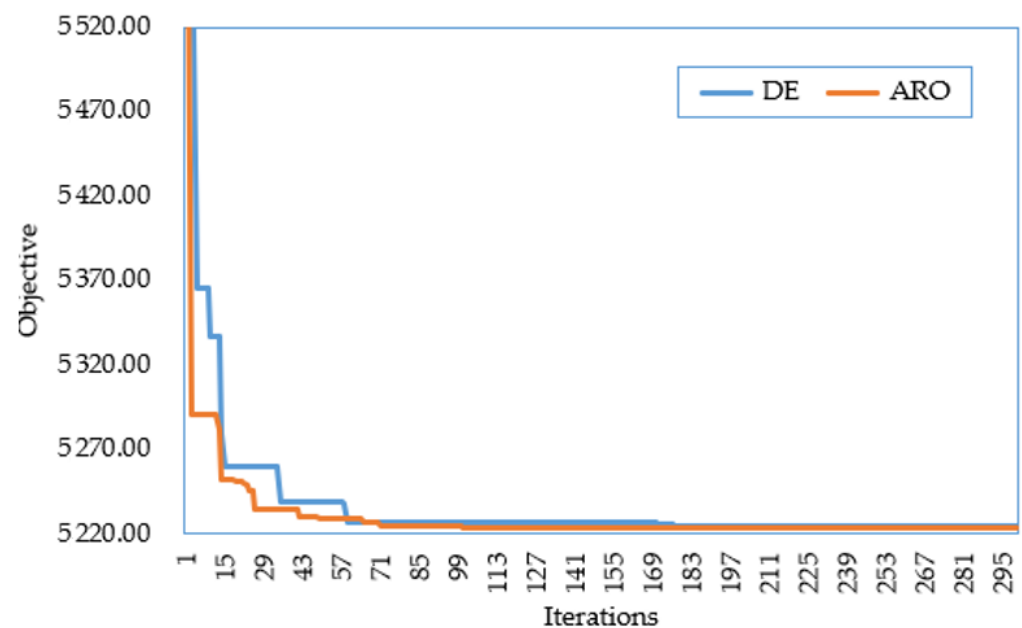
Figure 8. Convergence characteristics of DE and the AROA for the second scenario for the IEEE 33-distribution system.

From Table 2, the energy losses, voltage deviations, and their corresponding objectives obtained by the proposed AROA, without any violations, are 2482.624 kWh/day, 28.4663 p.u./day, and 5223.662, respectively, with violation of 2712.6, whilst the obtained results of DE are 2485.314 kWh/day, 28.4277 p.u./day, and 5224.216, respectively, with violation of 2710.4729.

It can be observed from Table 2 that the objectives of the proposed AROA and DE are reduced to 5223.662 and 5224.216 compared with the initial value of 10,505.6. As shown, the constraint violations have been greatly reduced from 6912.71 to 2710.47 and 2712.6 using DE and AROA. This improvement in the constraint violations represent 60% approximately. On the other side, the PV distributed energy sources operating at unity power factor are not

sufficient to achieve all the constraints all over the day since there are a significant number of constraint violations.

Figure 9 illustrates the hourly active power losses for this scenario compared to the initial scenario. As shown, the power losses are greatly decreased, especially in the hours of high solar irradiations. At peak consumption hour of 14:00 p.m., the active power losses are highly reduced from 211 kW and 91.39 kW with 56.68% improvement. Additionally, Figure 10 displays the hourly voltage deviations for this scenario compared to the initial scenario. As shown, the voltage deviations are significantly decreased in the hours of high solar irradiations. At 14:00 p.m., the active power losses are highly reduced from 1.8118 and 1.07 p.u. with 40.89% improvement. Despite these improvements in the voltage deviations in the irradiation hours, the voltage profile still suffers from the decrease. To show that, Figure 11 describes the hourly voltage profile at all distribution nodes. As shown, the worst voltage profile occurred during the peak loading conditions where the nodes 8–18 and 27–33 suffered from undervoltage, compared to the minimum limit of 95%. At peak consumption hours, the lowest voltage on the grid is 0.9131 p.u. and occurs at bus 18.
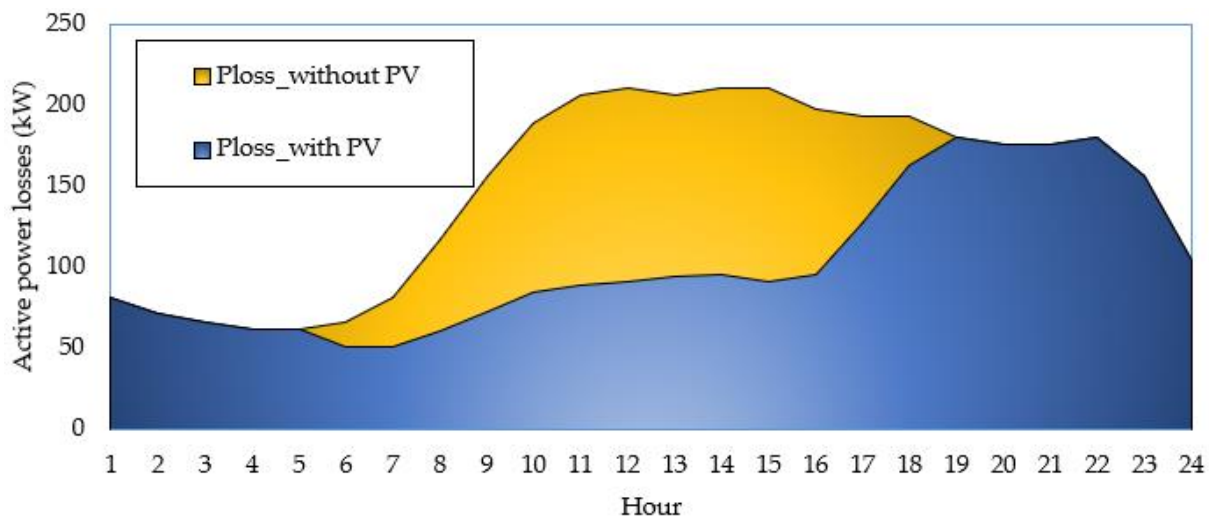

Figure 9. Hourly active power losses for the second scenario compared to the first scenario for the IEEE 33-distribution system.
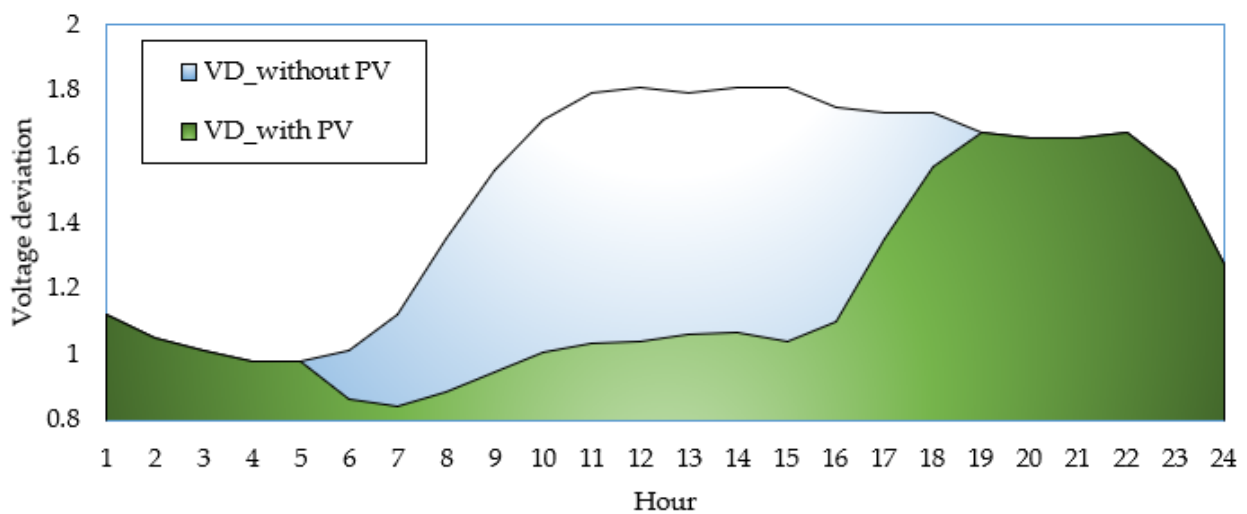

Figure 10. Hourly voltage deviations for the second scenario compared to the first scenario for the IEEE 33-distribution system.
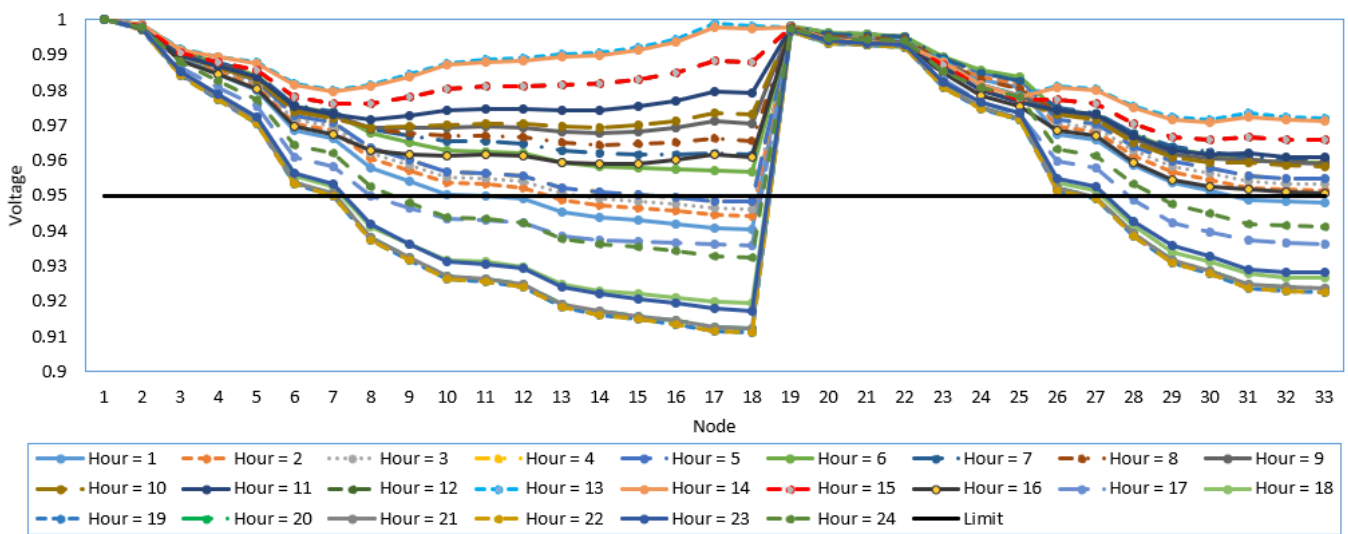
Figure 11. Hourly voltage profile for the second for the IEEE 33-distribution system.

These drawbacks clearly demonstrate the importance of reactive power support requirements which can be achieved using PVSTATCOM as described in the following scenario.

4.3. Third Scenario

In this scenario, the proposed AROA is applied in comparison to DE for PV allocations, with STATCOM, to minimize the considered objective function (Equation (23)). Additionally, a recent optimization method is expanded for comparison with the golden search optimization (GSO) algorithm [42]. Therefore, the proposed AROA, DE, and GSO are applied for this scenario where Figure 12 displays the convergence characteristics of GSO, DE, and the AROA for scenario 3. The figure shows that the AROA has excellent convergence characteristics compared with GSO and DE in obtaining the least objective of PVSTATCOM. Additionally, Table 3 shows that the allocations of PV with STATCOM for this scenario, where the numbers of installed buses obtained by the AROA are 7, 14, and 31, and their corresponding PV sizes are 652, 969, and 830 kW, respectively, and their corresponding STATCOM sizes are ±862, ±769, and ±838 kVAr, respectively. In addition to this, the numbers of installed buses obtained by DE are 31, 15, and 8, and their corresponding PV sizes are 934, 448, and 716 kW, respectively, and their corresponding STATCOM sizes are ±953, ±965, and ±842 kVAr, respectively. It can be noticed from this table that the objective of the proposed AROA is reduced to 1643.77 compared with 2132.16 that is achieved from the DE. This result shows a great improvement of 22.9% based on the proposed AROA compared to the DE. Moreover, the numbers of installed buses obtained by GSO are 10, 32, and 33, and their corresponding PV sizes are 1000, 451, and 1000 kW, respectively, and their corresponding STATCOM sizes are ±1000, ±1000, and ±1000 kVAr, respectively. It can be noticed from this table that the objective of the proposed AROA is reduced to 1643.77 compared with 2387.5 that is achieved via GSO. This result shows a great improvement of 31.15% based on the proposed AROA compared to GSO.

From Table 3, the sizing of STACOM are "±" where it can absorb and inject reactive powers to the system. Therefore, the values reported in the tables are the maximum size which is the rating value that may be absorbed or injected based on the operating condition.
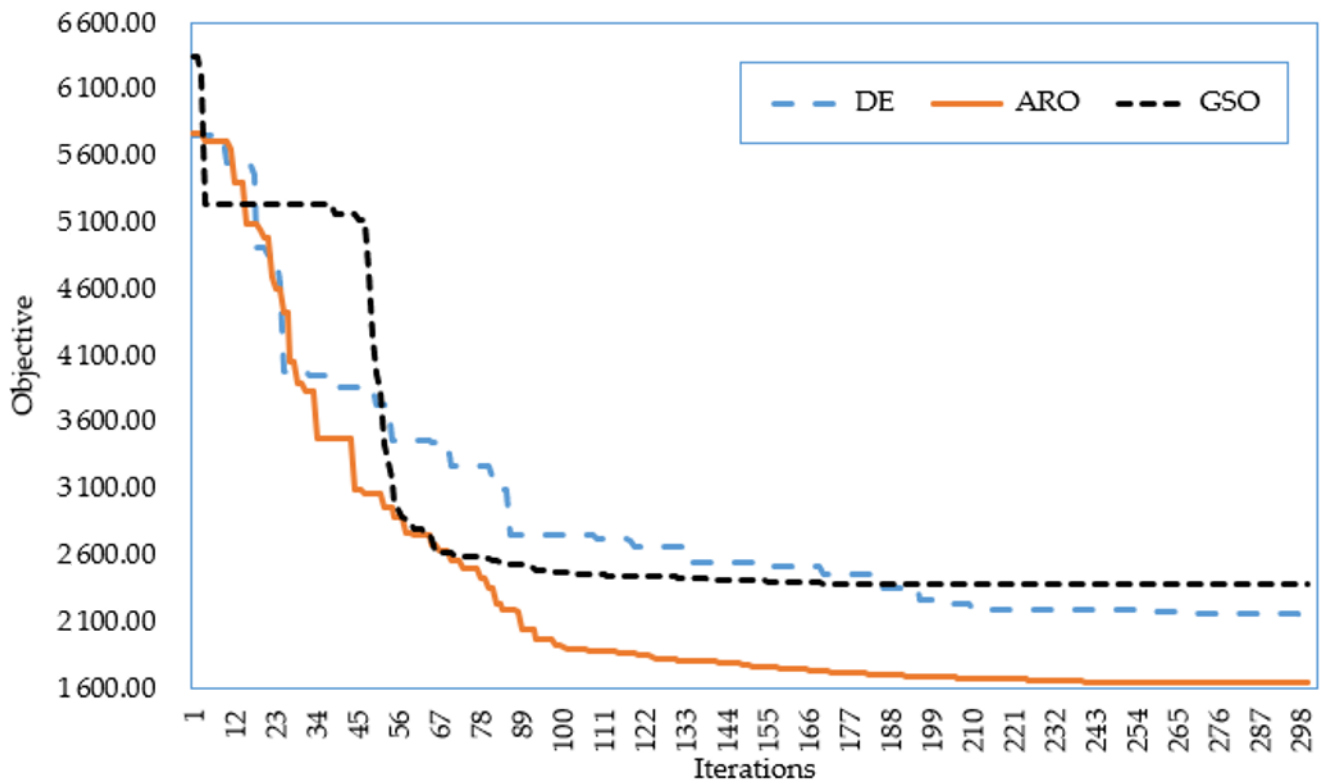
Figure 12. Convergence characteristics of DE and the AROA for the third scenario for the IEEE 33-distribution system.

Table 3. Allocations of PV with STATCOM for the third scenario for the IEEE 33-distribution system.

Items	GSO	DE	AROA
	10	31	7
Installed buses	32	15	14
	33	8	31
	1000	934	652
Regarding PV Size (kW)	451	448	969
	1000	716	830
	±1000	±953	±862
Regarding (kVAr)	±1000	±965	±769
	±1000	±842	±838
Objective	2387.5	2132.1595	1643.774

To illustrate the comparison between the AROA, GSO, and DE, the energy losses, voltage deviations, violations, their corresponding objectives are developed for this scenario as depicted in Table 4. As shown, based on the proposed AROA, the energy losses are greatly reduced from 3557.2479 kWh/day at the initial scenario to 1623.56 kWh/day with 54.36% reduction. Moreover, based on the proposed AROA, the voltage deviations are greatly reduced from 35.643 p.u./day at the initial scenario to 20.21 p.u./day with 43.29%. Moreover, the proposed AROA provides no violations in all constraints while DE and GSO fail to achieve these limits maintain. Therefore, the proposed AROA shows greater dependability than DE and GSO.

Table 4. Corresponding energy losses, voltage deviations, and violations for the third scenario for the IEEE 33-distribution system.

Items	Initial	GSO	DE	AROA
Energy Losses (kWh/day)	3557.2479	2111.2	1979.7587	1623.56
Voltage deviations (p.u./day)	35.643	21.6216	23.03956	20.2141
Violations	6912.71	254.7555	129.36121	0
Objective	10505.6	2387.5	2132.1595	1643.774

For this scenario, Figure 13 describes the hourly voltage profile of all distribution nodes for each loading hour. It is apparent from this figure that all voltage profiles are more than the minimum limit of 95%. At peak consumption hours, the lowest voltage on the grid is 0.95 p.u. and occurs at bus 18, as shown in Figure 13.
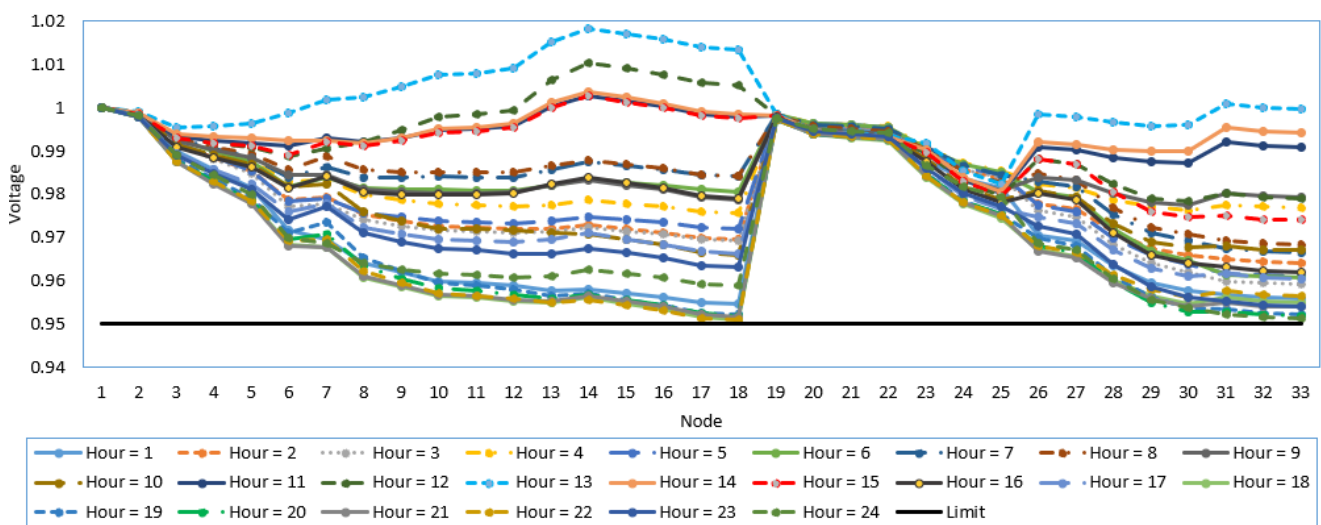

Figure 13. Hourly voltage profile for the third scenario for the IEEE 33-distribution system.

Furthermore, Figure 14 offers the hourly voltage deviations for this scenario compared to the other scenarios. This figure clearly illustrates the great improvement in the voltage profile in all hours. Moreover, Figure 15 illustrates the hourly active power losses for this scenario compared to the other scenarios. As shown, the power losses are greatly decreased in all loading hours.
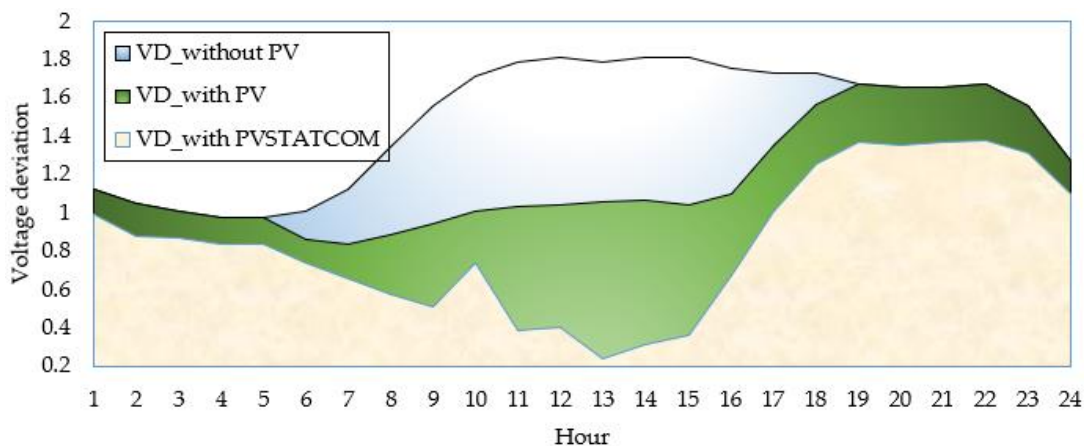

Figure 14. Hourly voltage deviations for the third scenario compared to the first and second scenarios for the IEEE 33-distribution system.
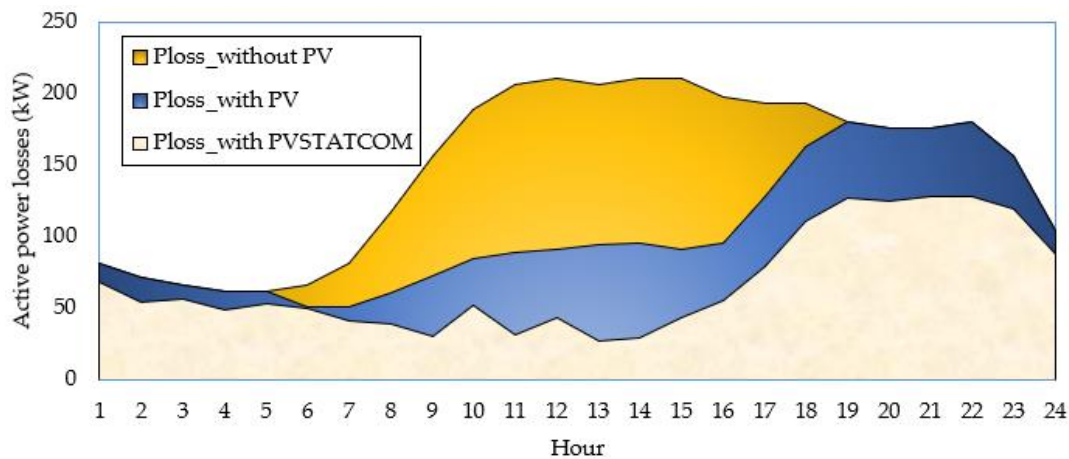
Figure 15. Hourly active power losses for the third scenario compared to the first and second scenarios for the IEEE 33-distribution system.

To compare the convergence time in seconds/minutes of the three algorithms, the average computational times in seconds of the AROA, GSO, and DE are recorded in Table 5. As shown, the proposed AROA has the fastest speed with the smallest computation time of 531.833 s. The proposed AROA is 29.92% faster than GSO and 9.16% faster than DE.

Table 5. Average computational times of the AROA, GSO, and DE for the third scenario for the IEEE 33-distribution system.

Items	GSO	DE	AROA
Computational Time (second)	758.85	585.51	531.833

5. Conclusions

In this article, the artificial rabbits' optimization algorithm (AROA) is developed for minimizing both the daily voltage profile and the daily energy losses, taking into consideration different 24 h loadings. The novel AROA is conducted for allocation of individual PV distributed energy resources and simultaneous PVSTATCOM to minimize the considered objective function through the 24 h daily horizon. The effectiveness of the proposed AROA is demonstrated in comparison to the differential evolution (DE) algorithm and the golden search optimization (GSO) algorithm. The higher effectiveness of the proposed AROA versus DE and GSO in minimizing the energy losses and voltage profile deviations and maintaining all the operational constraints was demonstrated. Added to that, PV sources are not sufficient to achieve all the constraints all over the day since there are a significant number of constraint violations. Moreover, the reactive power support via PVSTATCOM based on the proposed AROA provides great improvement to the distribution system by achieving the minimum energy losses and improving the voltage profile all over the daytime hours. According to the convergence characteristics, the suggested AROA can find a precise solution in a short time compared to DE and GSO. The PVSTATCOM, which was sized to meet the need for compensation at the time of maximum voltage violation, was adequate to fulfil the needs of reactive compensation at other times of the day. Throughout the day, the PVSTATCOM was able to execute reactive compensation while still performing its primary active power generation function. The suggested AROA can aid in the allocation, sizing, and planning of PVSTATCOMs that will provide reactive compensation. They could be implemented by utilities or industry investors.

References

1. International Energy Agency. *Renewables 2020—Analysis*; IEA: Paris, France, 2020.
2. Jay, D.; Swarup, K.S. A comprehensive survey on reactive power ancillary service markets. *Renew. Sustain. Energy Rev.* **2021**, *144*, 110967. [CrossRef]
3. Wolgast, T.; Ferenz, S.; Nieße, A. Reactive Power Markets: A Review. *IEEE Access* **2022**, *10*, 28397–28410. [CrossRef]
4. El-Ela, A.A.A.; El-Sehiemy, R.A.; Shaheen, A.M.; Ellien, A.R. Review on Active Distribution Networks with Fault Current Limiters and Renewable Energy Resources. *Energies* **2022**, *15*, 7648. [CrossRef]
5. Ginidi, A.R.; Shaheen, A.M.; El-Sehiemy, R.A.; Hasanien, H.M.; Al-Durra, A. Estimation of electrical parameters of photovoltaic panels using heap-based algorithm. *IET Renew. Power Gener.* **2022**, *16*, 2292–2312. [CrossRef]
6. Shaheen, A.M.; Elsayed, A.M.; Ginidi, A.R.; El-Sehiemy, R.A.; Elattar, E. Enhanced social network search algorithm with powerful exploitation strategy for PV parameters estimation. *Energy Sci. Eng.* **2022**, *10*, 1398–1417. [CrossRef]
7. Eslami, M.; Akbari, E.; Sadr, S.T.S.; Ibrahim, B.F. A novel hybrid algorithm based on rat swarm optimization and pattern search for parameter extraction of solar photovoltaic models. *Energy Sci. Eng.* **2022**, *10*, 2689–2713. [CrossRef]
8. Yaghoubi, M.; Eslami, M.; Noroozi, M.; Mohammadi, H.; Kamari, O.; Palani, S. Modified Salp Swarm Optimization for Parameter Estimation of Solar PV Models. *IEEE Access* **2022**, *10*, 110181–110194. [CrossRef]
9. Cui, Z.; Kang, L.; Li, L.; Wang, L.; Wang, K. A combined state-of-charge estimation method for lithium-ion battery using an improved BGRU network and UKF. *Energy* **2022**, *259*, 124933. [CrossRef]
10. Li, D.; Yang, D.; Li, L.; Wang, L.; Wang, K. Electrochemical Impedance Spectroscopy Based on the State of Health Estimation for Lithium-Ion Batteries. *Energies* **2022**, *15*, 6665. [CrossRef]
11. Elshahed, M. Assessment of sudden voltage changes and flickering for a grid-connected photovoltaic plant. *Int. J. Renew. Energy Res.* **2016**, *6*, 1328–1335. [CrossRef]
12. Elshahed, M. Complying grid-connected wind farm according to the requirements of utility grid code using STATCOM. In Proceedings of the 2017 9th IEEE-GCC Conference and Exhibition, Manama, Bahrain, 8–11 May 2017.
13. International Electrotechnical Commission. *IEC 60050 International Electrotechnical Vocabulary—Details for IEV Number 617-01-05*; IEC: Geneva, Switzerland, 2009.
14. Kotsampopoulos, P.; Hatziargyriou, N.; Bletterie, B.; Lauss, G. Review, analysis and recommendations on recent guidelines for the provision of ancillary services by Distributed Generation. In Proceedings of the 2013 IEEE International Workshop on Intelligent Energy Systems (IWIES), Vienna, Austria, 14 November 2013.
15. Braun, M. *Provision of Ancillary Services by Distributed Generators*; Kassel University Press: Kassel, Germany, 2008; Volume 10.
16. Gawhade, P.; Ojha, A. Recent advances in synchronization techniques for grid-tied PV system: A review. *Energy Rep.* **2021**, *7*, 6581–6599. [CrossRef]
17. Xavier, L.S.; Cupertino, A.F.; Pereira, H.A. Ancillary services provided by photovoltaic inverters: Single and three phase control strategies. *Comput. Electr. Eng.* **2018**, *70*, 102–121. [CrossRef]
18. Magdy, M.; Elshahed, M.; Ibrahim, D.K. Enhancing PV Hosting Capacity Using Smart Inverters and Time of Use Tariffs. *Iran. J. Sci. Technol. Trans. Electr. Eng.* **2021**, *45*, 905–920. [CrossRef]
19. Rivera, D.; Guillen, D.; Mayo-Maldonado, J.C.; Valdez-Resendiz, J.E.; Escobar, G. Power grid dynamic performance enhancement via statcom data-driven control. *Mathematics* **2021**, *9*, 2361. [CrossRef]
20. Varma, R.K.; Khadkikar, V.; Seethapathy, R. Nighttime application of PV solar farm as STATCOM to regulate grid voltage. *IEEE Trans. Energy Convers.* **2009**, *24*, 983–985. [CrossRef]
21. Varma, R.K.; Khadkikar, V.; Rahman, S.A. Utilization of Distributed Generator Inverters as STATCOM. U.S. Patent 9,325,173, 26 April 2016.
22. Varma, R.K.; Siavashi, E.M. PV-STATCOM: A New Smart Inverter for Voltage Control in Distribution Systems. *IEEE Trans. Sustain. Energy* **2018**, *9*, 1681–1691. [CrossRef]
23. Varma, R.K.; Siavashi, E.M. Enhancement of solar farm connectivity with smart PV inverter PV-STATCOM. *IEEE Trans. Sustain. Energy* **2019**, *10*, 1161–1171. [CrossRef]

24. Varma, R.K.; Siavashi, E.; Mohan, S.; McMichael-Dennis, J. Grid Support Benefits of Solar PV Systems as STATCOM (PV-STATCOM) through Converter Control: Grid Integration Challenges of Solar PV Power Systems. *IEEE Electrif. Mag.* **2021**, *9*, 50–61. [CrossRef]
25. Varma, R.K.; Maleki, H. PV Solar System Control as STATCOM (PV-STATCOM) for Power Oscillation Damping. *IEEE Trans. Sustain. Energy* **2019**, *10*, 1793–1803. [CrossRef]
26. Popavath, L.N.; Kaliannan, P. Photovoltaic-STATCOM with low voltage ride through strategy and power quality enhancement in a grid integrated Wind-PV system. *Electronics* **2018**, *7*, 51. [CrossRef]
27. Luo, L.; Gu, W.; Zhang, X.P.; Cao, G.; Wang, W.; Zhu, G.; You, D.; Wu, Z. Optimal siting and sizing of distributed generation in distribution systems with PV solar farm utilized as STATCOM (PV-STATCOM). *Appl. Energy* **2018**, *210*, 1092–1100. [CrossRef]
28. Luo, L.; Wu, Z.; Gu, W.; Huang, H.; Gao, S.; Han, J. Coordinated allocation of distributed generation resources and electric vehicle charging stations in distribution systems with vehicle-to-grid interaction. *Energy* **2020**, *192*, 116631. [CrossRef]
29. Rezaeian-Marjani, S.; Galvani, S.; Talavat, V.; Farhadi-Kangarlu, M. Optimal allocation of D-STATCOM in distribution networks including correlated renewable energy sources. *Int. J. Electr. Power Energy Syst.* **2020**, *122*, 106178. [CrossRef]
30. Shaheen, A.M.; Elattar, E.E.; El-Sehiemy, R.A.; Elsayed, A.M. An Improved Sunflower Optimization Algorithm-Based Monte Carlo Simulation for Efficiency Improvement of Radial Distribution Systems Considering Wind Power Uncertainty. *IEEE Access* **2021**, *9*, 2332–2344. [CrossRef]
31. Kumar, P.; Bohre, A.K. Optimal Allocation of Solar-PV and STATCOM Using PSO with Multi-Objective Approach to Improve the Overall System Performance. In *Lecture Notes in Electrical Engineering*; Springer: Berlin/Heidelberg, Germany, 2022; Volume 812.
32. Kumar, P.; Bohre, A.K. Optimal allocation of Hybrid Solar-PV with STATCOM based on Multi-objective Functions using combined OPF-PSO Method. In Proceedings of the International Conference on IoT Based Control Networks & Intelligent Systems (ICICNIS), Kottayam, India, 28–29 June 2021. [CrossRef]
33. Wang, L.; Cao, Q.; Zhang, Z.; Mirjalili, S.; Zhao, W. Artificial rabbits optimization: A new bio-inspired meta-heuristic algorithm for solving engineering optimization problems. *Eng. Appl. Artif. Intell.* **2022**, *114*, 105082. [CrossRef]
34. Gasperic, S.; Mihalic, R. Estimation of the efficiency of FACTS devices for voltage-stability enhancement with PV area criteria. *Renew. Sustain. Energy Rev.* **2019**, *105*, 144–156. [CrossRef]
35. Varma, R.K.; Das, B.; Axente, I.; Vanderheide, T. Optimal 24-hr utilization of a PV solar system as STATCOM (PV-STATCOM) in a distribution network. In Proceedings of the 2011 IEEE Power and Energy Society General Meeting, Detroit, MI, USA, 24–28 July 2011.
36. Sadiq, R.; Wang, Z.; Chung, C.Y.; Zhou, C.; Wang, C. A review of STATCOM control for stability enhancement of power systems with wind/PV penetration: Existing research and future scope. *Int. Trans. Electr. Energy Syst.* **2021**, *31*, e13079. [CrossRef]
37. Sirjani, R. Optimal placement and sizing of PV-STATCOM in power systems using empirical data and adaptive particle swarm optimization. *Sustainability* **2018**, *10*, 727. [CrossRef]
38. Nasef, A.; Shaheen, A.; Khattab, H. Local and remote control of automatic voltage regulators in distribution networks with different variations and uncertainties: Practical cases study. *Electr. Power Syst. Res.* **2022**, *205*, 107773. [CrossRef]
39. Shaheen, A.M.; Elsayed, A.M.; El-Sehiemy, R.A.; Kamel, S.; Ghoneim, S.S.M. A modified marine predators optimization algorithm for simultaneous network reconfiguration and distributed generator allocation in distribution systems under different loading conditions. *Eng. Optim.* **2021**, *54*, 687–708. [CrossRef]
40. Shaheen, A.; El-Sehiemy, R.; Kamel, S.; Selim, A. Optimal Operational Reliability and Reconfiguration of Electrical Distribution Network Based on Jellyfish Search Algorithm. *Energies* **2022**, *15*, 6994. [CrossRef]
41. El-Ela, A.; Abou El-Ela, A.A.; El-Sehiemy, R.A.; Allam, S.M.; Shaheen, A.M.; Nagem, N.A.; Sharaf, A.M. Renewable Energy Micro-Grid Interfacing: Economic and Environmental Issues. *Electronics* **2022**, *11*, 815. [CrossRef]
42. Noroozi, M.; Mohammadi, H.; Efatinasab, E.; Lashgari, A.; Eslami, M.; Khan, B. Golden Search Optimization Algorithm. *IEEE Access* **2022**, *10*, 37515–37532. [CrossRef]